JOURNAL OF GEOPHYSICAL RESEARCH, VOL. 112, A06321, doi:10.1029/2006JA012051, 2007

Imaging coherent scatter radar, incoherent scatter radar, and optical observations of quasiperiodic structures associated with sporadic *E* layers

M. F. Larsen,[1] D. L. Hysell,[2] Q. H. Zhou,[3] S. M. Smith,[4] J. Friedman,[5] and R. L. Bishop[6]

Received 1 September 2006; revised 17 January 2007; accepted 14 March 2007; published 20 June 2007.

[1] During June and July 2002, a 30-MHz imaging coherent scatter radar was installed and operated on the island of St. Croix, to view the *E* region ionosphere above Arecibo, Puerto Rico. During the observing period, 10 events with discernible quasiperiodic echo structure were observed with the coherent scatter radar. In six of those events, simultaneous measurements were made with the Arecibo 430-MHz incoherent scatter radar. The imaging coherent scatter radar allows us to locate and track the echo structures within the volume illuminated by the transmitter, which shows structures that are generally aligned along wavefronts. A slight preference for motion of the structures toward the southwest is evident throughout the period, but the propagation directions and speeds vary greatly. The incoherent scatter radar measurements show a close correspondence between the occurrence of the coherent echoes and the location of the enhanced electron density structures. In particular, the coherent echoes occur when the electron density layers show uplifts.

Citation: Larsen, M. F., D. L. Hysell, Q. H. Zhou, S. M. Smith, J. Friedman, and R. L. Bishop (2007), Imaging coherent scatter radar, incoherent scatter radar, and optical observations of quasiperiodic structures associated with sporadic *E* layers, *J. Geophys. Res.*, *112*, A06321, doi:10.1029/2006JA012051.

1. Introduction

[2] In this paper, we summarize the observations of sporadic *E* layers and quasiperiodic (QP) echoes made during a 3-week period in the Caribbean in June and July 2002. The data set includes measurements made with an incoherent scatter radar, an imaging coherent scatter radar, an optical imaging system, and a lidar. We therefore have common volume measurements of the background plasma, the plasma structure and its motion, and the neutral structure and its motion. In this respect, the experiment provides a much more complete picture of the environment associated with QP echoes than has typically been available in earlier experiments.

[3] A 30-MHz radar with multiple receivers and multiple receiving antenna baselines was installed on the island of St. Croix. The transmitting and receiving arrays were pointed toward the west-northwest in the direction toward Puerto Rico. The requirement for backscatter to occur is that the beam direction is perpendicular to the magnetic field lines. The locus of points in the lower *E* region defined in this way included a broad area over the western half of Puerto Rico that included the volume that can be sampled with the Arecibo 430-MHz incoherent scatter radar. The basic parameters of the experiment, the basic principles of the imaging radar technique, and the first results from one night of observations when particularly strong echoes were detected over Puerto Rico have been described by *Hysell et al.* [2004]. The geometry is shown in Figure 1.

[4] The most commonly recognized indication of the presence of QP echo structure is also the feature that was first used by *Yamamoto et al.* [1991, 1992] to identify the phenomenon, namely, lines of echoes in the range-time-intensity (RTI) plots with negative slopes, i.e., slopes toward the radar. Typical periodicities between adjacent lines of echoes were found to be in the range of a few minutes to as much as 10 min in some cases. Although the initial observations suggested a consistent negative slope, subsequent observations showed both positive and negative slopes and a tendency for the slopes to reverse during the night [see, e.g., *Hysell and Burcham*, 1999; *Pan and Larsen*, 2000]. Furthermore, the imaging coherent scatter radar observations from St. Croix that were described in the earlier paper [*Hysell et al.*, 2004] showed clearly that patterns in the RTIs that appear simple often mask a more complicated pattern of echolocations and echo scattering center movements in three-dimensional space.

[5] The common volume observations with the Arecibo UHF incoherent scatter radar (ISR) and the St. Croix HF imaging coherent scatter radar (CSR) provide a unique view

[1]Department of Physics and Astronomy, Clemson University, Clemson, South Carolina, USA.
[2]Earth and Atmospheric Sciences, Cornell University, Ithaca, New York, USA.
[3]Electrical and Computer Engineering Department, Miami University, Oxford, Ohio, USA.
[4]Center for Space Physics, Boston University, Boston, Massachusetts, USA.
[5]The Arecibo Observatory, Arecibo, Puerto Rico.
[6]The Aerospace Corporation, Los Angeles, California, USA.

0148-0227/07/2006JA012051$09.00

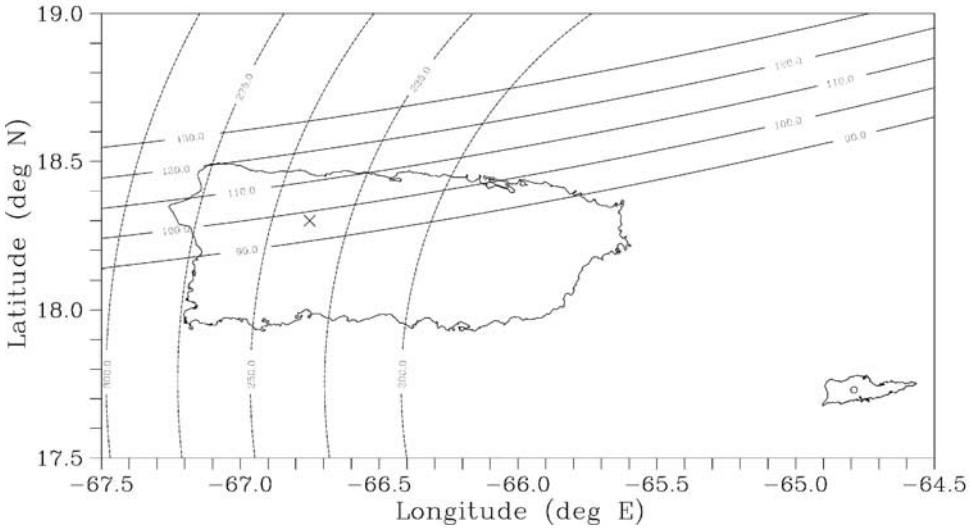

Figure 1. Map shows the locations of the coherent scatter imaging radar on St. Croix and the incoherent scatter radar at Arecibo, Puerto Rico. Concentric dashed circles indicate the distance from the radar on St. Croix to a point on the circle at 100-km altitude. Horizontal curves represent the locus of perpendicularity from St. Croix at different altitudes.

of the processes and dynamics associated with QP echoes. The ISR backscatter shows the electron density structures directly, and by scanning in azimuth, information about the horizontal and vertical gradients in that structure can be obtained. The CSR backscatter requires perpendicularity of the beam to the magnetic field lines and the presence of plasma structure at the scale size of half the radar wavelength. Some enhancement in the electron densities clearly has to be present as well to produce coherent scatter, but it is not necessarily the case that the backscatter occurs where the largest density enhancements are found. The combination of the ISR and CSR measurements can be used to examine the relationship between the two.

[6] Besides the ISR, the Arecibo Observatory also has considerable optical instrumentation, including a resonance lidar and imagers operating at several different wavelengths. On one of the nights when QP echoes were observed with the CSR, we were also able to obtain potassium lidar and 557.7- and 630.0-nm all-sky imager data.

[7] In the remainder of the paper we will focus on the data from three nights of observations during the 3-week period.

2. Observations

2.1. 14 June 2002

[8] One of the most active nights with QP echoes occurred at the beginning of the 3-week observing period on 14 June 2002. The RTI plot obtained with the CSR on St. Croix is shown in Figure 2. Throughout the night, there was a mixture of positive and negative, i.e., toward and away, slopes in the QP echo structures. In the period prior to 0015 UT [2015 Atlantic standard time (AST)], both slopes occurred in the same time period throughout the range where echoes were observed. From 0015 UT to approximately 0030 UT there is a period with predominantly positive slopes. Later, between 0115 and 0200 UT, there is a period when the slopes are more uniform with predominantly toward slopes, especially in the range from 240 to 280 km. This data set was described in more detail by *Hysell et al.* [2004].

[9] The map of the scatterers derived from the imaging analysis at 0038 UT (2038 AST) is shown in Figure 3. All references to local time here and in the remainder of the paper refer to AST. Four bands of echoes, two bright bands and two weaker bands further to the north and south, can be seen in the figure aligned roughly from west-northwest to east-southeast. A similar analysis was carried out for each set of measurements in the time sequence so that a movie could be made to show the propagation direction and velocity of the structures, as well as their time evolution. The image sequence shows that the bands were propagating in the south-southwest direction, roughly perpendicular to the alignment of the bands. The observed propagation direction at this time was consistent with the preferred direction inferred in some earlier studies, i.e., toward the southwest or south-southwest.

[10] On the night of 14 June, the Arecibo ISR was operated in a dual beam mode using both the Gregorian and line feeds. The two feeds are located on the same azimuth arm and are typically placed symmetrically with respect to zenith, as was the case in the observations described here. The beams were therefore 180° apart in azimuth. On this night and the other nights described later, the beams were pointed off vertical at a zenith angle of 15°. The radar was scanned continuously in azimuth throughout the observing period. The RTI obtained in this way is shown in Figure 4. The values plotted here, and in subsequent Arecibo RTIs, represent the pulse-to-pulse coherence, which is a proxy for relative power and thus also for the electron density. The measurements from the two different beam directions are shown in the same figure with red and green shading, respectively. The panel at the top of the figure shows the azimuth direction for each beam with the same red and green designation. The period required for a full 360° scan was approximately 30 min. The scans were

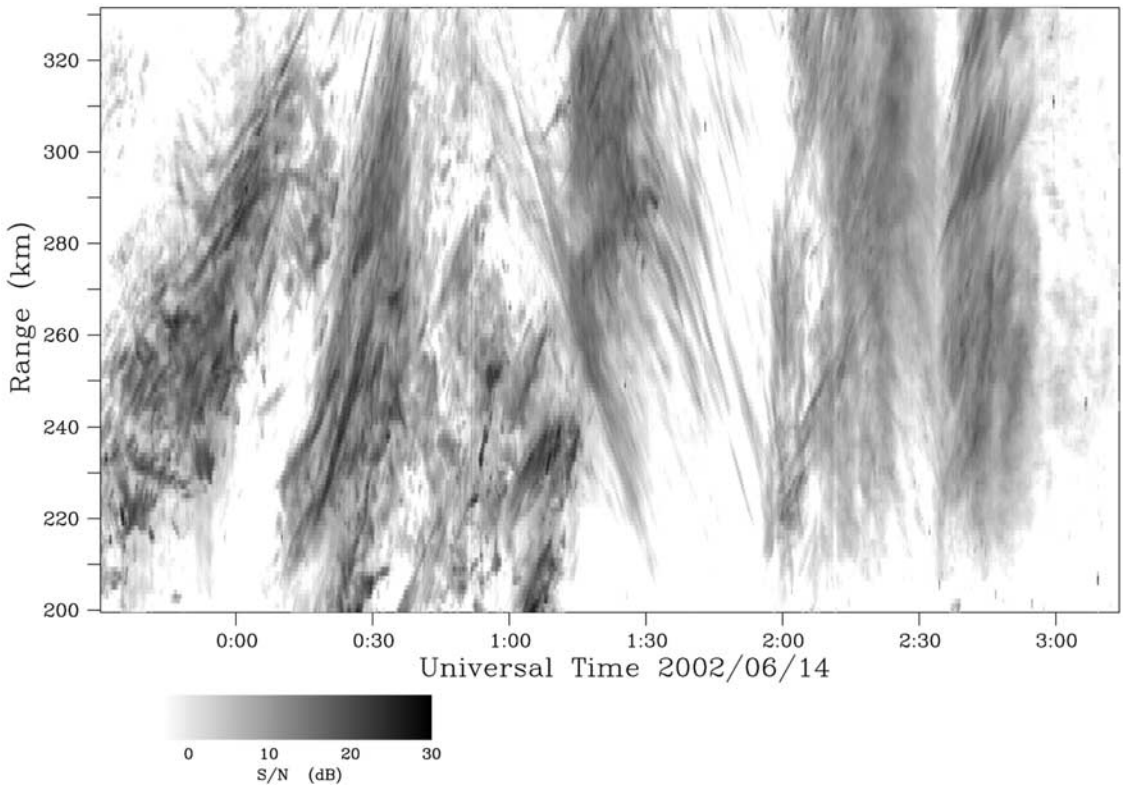

Figure 2. Coherent scatter radar RTI plot for the observations on the night of 14–15 June 2002. The radar was located on the island of St. Croix. The scattering region was above the island of Puerto Rico.

carried out in the clockwise and counterclockwise directions in alternate scan cycles.

[11] Comparing the red and green structures in the figure shows that the lags between similar structures detected in the two beams are primarily temporal rather than spatial. For example, around 2315 UT, similar structure is evident first in one beam, shown by the red shading, and then in the other beam, shown by the green shading. The delay, however, is less than the time required to complete a half scan cycle. The same applies to the structure that appears shortly after 0015. The uplift is seen first in the green shading and then in the red with a temporal lag much shorter than the time required for a 180° scan. The relationship between the measurements in the two beams is less clear after 0300 UT.

[12] Comparison of Figures 2 and 4 shows that there is a close correspondence between the periods when the uplift was observed and the occurrence of the QP echo structures. The first period with QP echoes was from approximately 2330 to 0015 UT. The second period was from 0015 UT to 0115 UT, and so on. After 0230 UT, it is difficult to identify slopes unambiguously in the CSR RTI plot. At the same

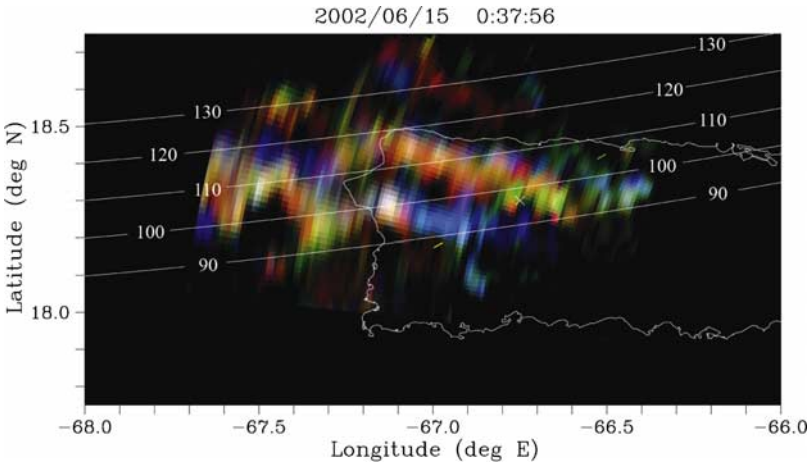

Figure 3. Map showing images obtained from the analysis of the coherent scatter measurements on 14 June 2002. The image in the figure corresponds to 0038 UT (AST + 4 hr).

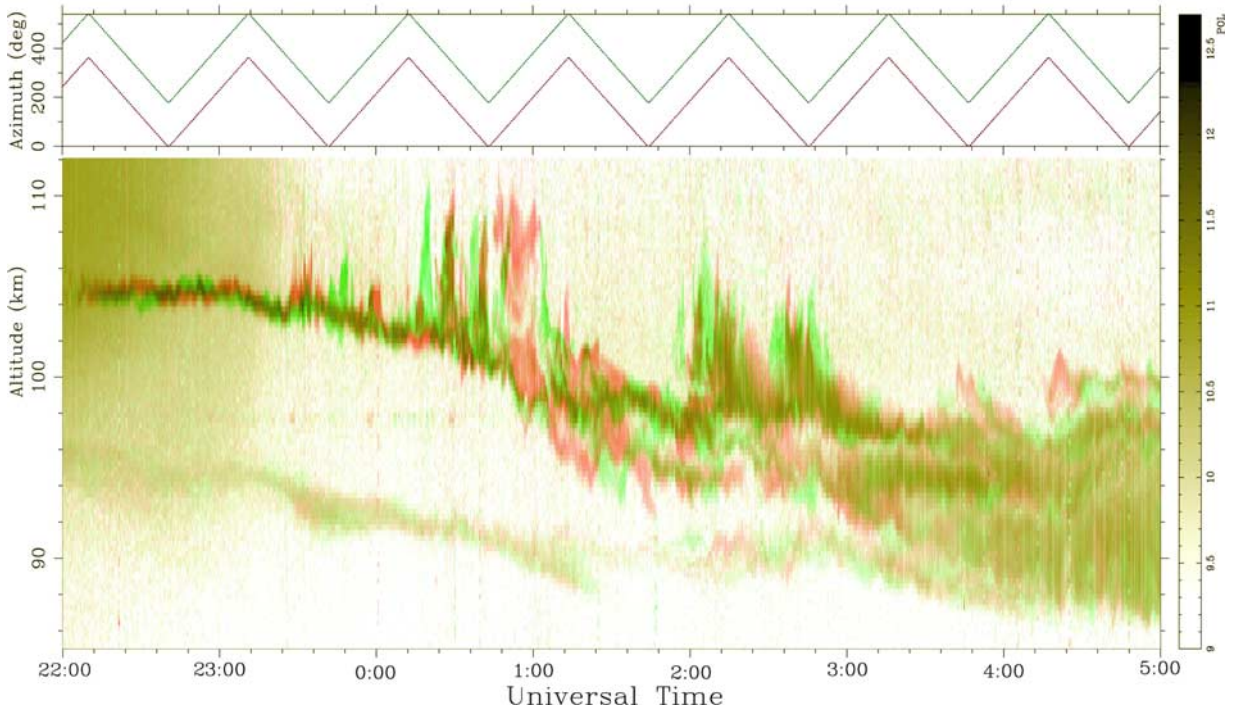

Figure 4. RTI measurements made with dual beams using the incoherent scatter radar at Arecibo. The measurements from one beam are indicated by the green shading and from the other by the red shading. The beam directions were swept in azimuth during the course of the observations. The pointing direction for each beam is shown in the upper panel.

time, it becomes difficult to identify the time lag between the structure observed in the two ISR beams, and the layer also becomes much broader in altitude extent.

[13] During the night of 14 June, the potassium resonance lidar was operated after 0130 UT (see Figure 5), which was after the first period of significant uplift prior to 0100 UT. The next major uplift occurred between approximately 0200 and 0300 UT. At that time the main potassium layer was located below 98-km altitude, but note the weaker potassium emissions that are visible above 105 km. In particular, there are two major uplifts in the sporadic *E* layer and two uplifts in the weak upper potassium layer that correspond both in timing and in duration. Figure 5 also shows that the upper potassium layer exhibited an upward displacement prior to the upward movement in the ionization layer that started at 0200 UT. The relationship between sporadic atom layers and sporadic ionization layers has been described in several earlier papers [e.g. *Kane et al.*, 2001], and a similar correspondence is evident here. The feature of more interest to us here, however, is the location of the weak sporadic potassium layer near the upper extent of the vertical displacement in the ionization layer, and particularly the occurrence of a strong upward displacement in the neutral layer before the first ionization uplift. The lidar measurements near 97-km altitude also showed a large temperature oscillation with an amplitude of 30 K between 0130 and 0330 UT, i.e., during the period when there are large layer uplifts. These large temperature fluctuations indicate that there were large vertical velocity fluctuations in the background neutral atmosphere during this period.

[14] At 0215 UT, the CSR image showed several bands of echoes located in the western half of Puerto Rico and extending into the region west of the island, as shown in Figure 6. On the night of 14 June, the Boston University all-sky imager system at Arecibo also provided data during part of the period covered by the radar data, including the time around 0215 UT. The system operates with four different filters, alternating between the four wavelengths and sampling each for 90 s. The effective sampling period for a single wavelength is therefore 6 min. The 557.7-nm green line is a neutral emission, of course, with a centroid emission altitude near 96 km. An image in 557.7-nm emission obtained at 0215 UT by the Boston University all-sky imager is shown in Figure 7. This is a time-difference image, i.e., the result from the subtraction of

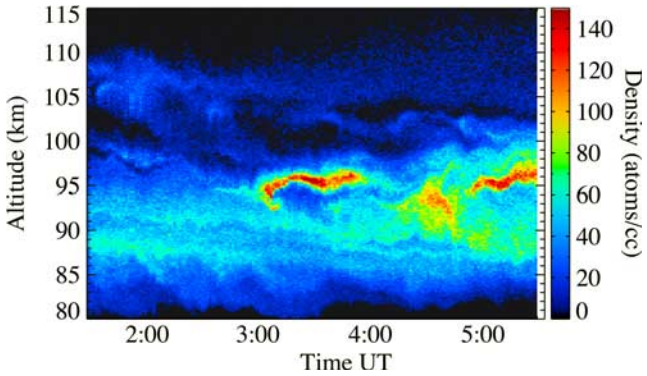

Figure 5. Lidar potassium density measurements made at Arecibo on the night of 14 June 2002.

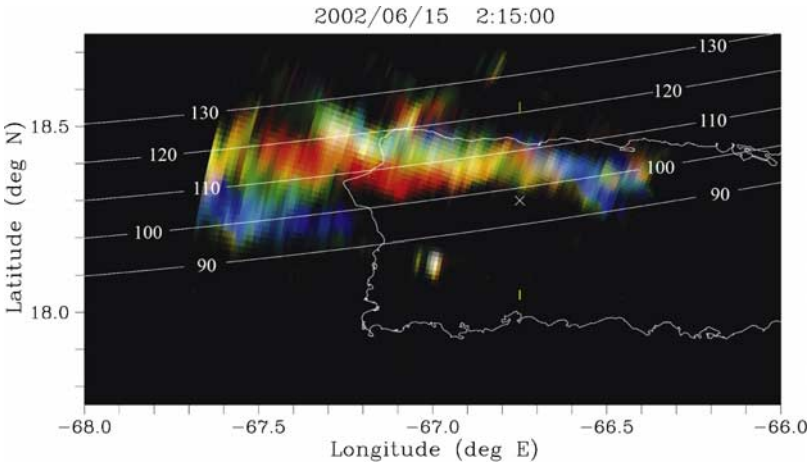

Figure 6. Map showing images obtained from the analysis of the coherent scatter measurements on 14 June 2002. The image in the figure corresponds to 0215 UT (AST + 4 hr).

two subsequent images, that has also been mapped onto the Earth's surface assuming an emission altitude of 96 km. The all-sky image includes coverage of a much larger area than that covered by the CSR, but similar structure is evident in the region that corresponds to the western part of Puerto Rico and the region west of the island. In fact, there is a one-to-one correspondence between the bands observed in the echo structure and the bands evident in the 557.7-nm emissions. The period of the waves in the radar images (Figure 6) is ~10 min, with a corresponding Nyquist sampling rate of 5 min. The green-line images were therefore undersampled. Movies of the optical imager data in fact show structure that appears to be propagating in a direction opposite to that of the structure in the radar images. When the undersampling is taken into account, however, the propagation phase speed and period are consistent in the two data sets. The 630.0-nm red-line imager data during the same period does not show any corresponding structure, indicating that the waves occur in the *E* region and not in the *F* region. A sequence of vertical displacements are also discernible in the potassium lidar data around that time, as can be seen in Figure 5 at the top of the potassium layer near 98- or 99-km altitude.

[15] *Taylor et al.* [1998] described observations of the OH and 557.7-nm emissions made with a pair of imaging systems located in Japan during the SEEK campaign when conventional coherent scatter radar measurements of QP echoes were also available. They found that the structures observed with the imagers were generally moving in directions that were centered around northeast. They concluded that there was no apparent relationship between those structures and the QP echo structures since the latter were found to be moving predominantly in the southwest direction, i.e., in the opposite direction. The effective sampling period for each imager wavelength in their experiment was similar to that used for the imager observations presented here. Detailed information about horizontal wavelengths and propagation speeds of the QP echo structures is not available in the paper of *Taylor et al.* [1998], but it seems likely that the general characteristics of the QP structures in their study were similar to those presented here and that the imager therefore undersampled the structures, as was the case in our observations. Undersampling could explain the apparent difference in the propagation directions between the radar and imager structures.

[16] Finally, we show the radar image map at 0059 UT (2059 AST) in Figure 8, which shows a series of echo structure bands aligned closer to the north-south direction in the region west of Puerto Rico. Those bands were observed to be propagating west to east, again approximately perpendicular to the orientation of the bands. In fact, during the observing period, a mixture of echo line orientations and propagation directions were observed. The overall data set is too small for any meaningful statistical analysis, but in general, there was a slight bias toward the west-northwest to east-southeast orientation with propagation toward south-

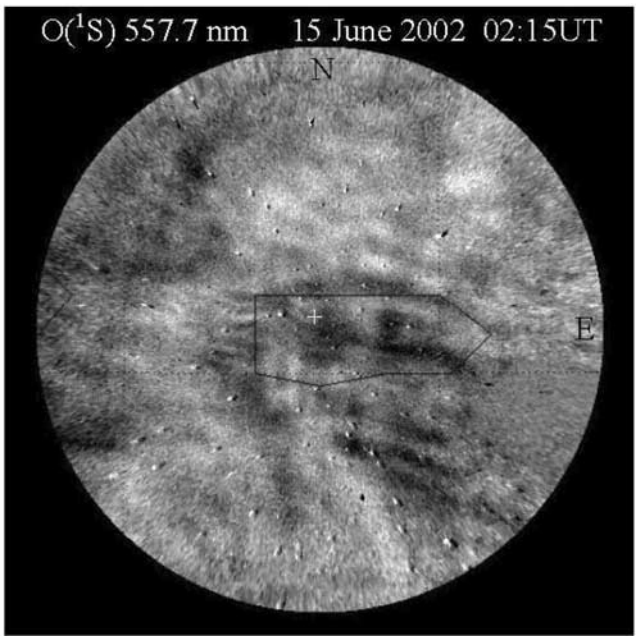

Figure 7. Time-difference all-sky image in 557.7-nm emission at 0215 UT on 15 June 2002. The image is shown as a negative image to highlight the wave structure.

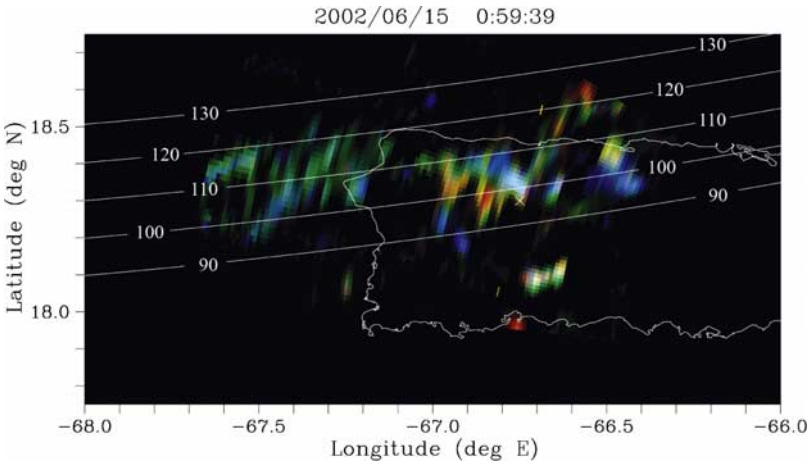

Figure 8. Map showing images obtained from the analysis of the coherent scatter measurements on 14 June 2002. The image in the figure corresponds to 0059 UT (AST + 4 hr).

southwest. A large fraction of the cases had other line orientations and propagation directions however.

2.2. 1 July 2002

[17] The night of 1 July 2002 had echoes that were comparable in magnitude to those on 14 June, although the active period was more limited in duration. The CSR RTI is shown in Figure 9, which shows a mixture of toward and away slopes in the lines of echoes throughout the periods of activity, with perhaps a tendency for more away slopes at the beginning of the night prior to 0030 UT (2030 AST) and a tendency toward more toward slopes after that time. Although lines of echoes are evident after 0200 UT (2200 AST), QP structure is more difficult to discern in the last period of activity.

[18] The ISR RTI for the night of 1 July is shown in Figure 10. At the beginning of the evening, the electron densities in the upper panel show three layers, a strong layer above 110 km and two weaker layers below 105 km. By 2230 UT, there are two strong layers. After 0130 UT, there are four distinct layers, one strong layer near 110 km and three weaker layers below 105 km. The data on 1 July were taken with a single beam direction, instead of the dual-beam setup used on 14 June and used a double pulse mode so that

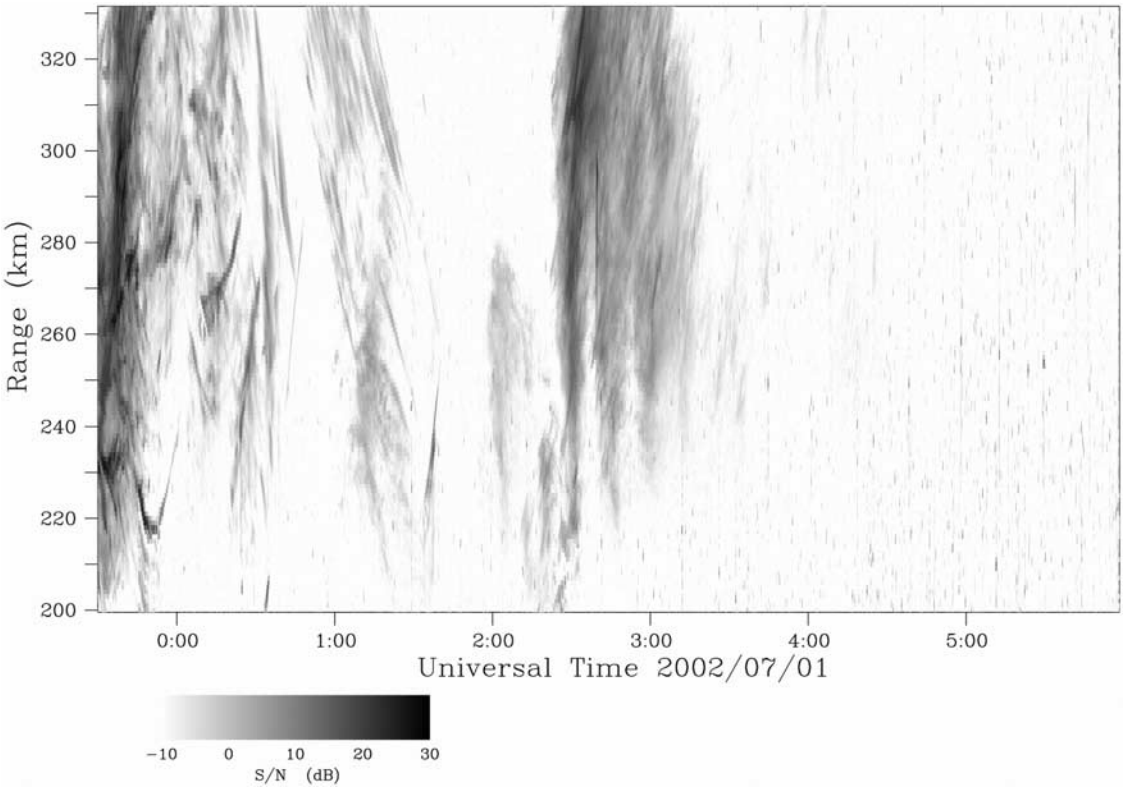

Figure 9. Coherent scatter radar RTI plot for the observations on the night of 1–2 July 2002.

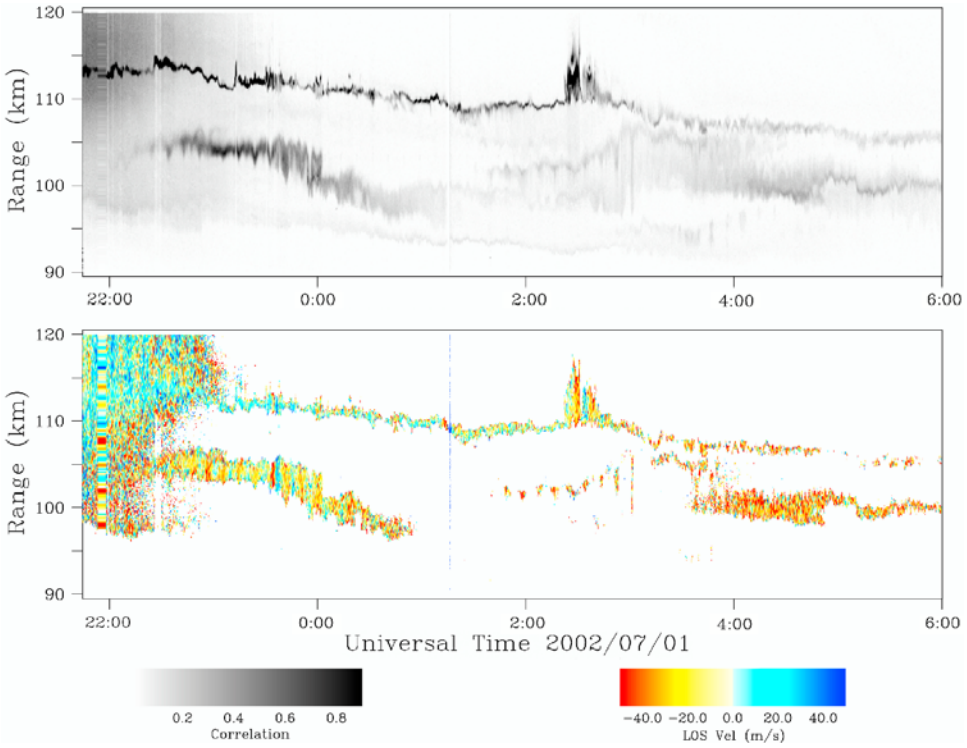

Figure 10. RTI measurements made with the incoherent scatter radar at Arecibo. The top panel shows the pulse-to-pulse coherence. The lower panel shows the Doppler velocity with positive velocities upward.

radial velocities could be measured. The velocities are shown in the lower panel of Figure 10. Velocity measurements are only possible when there are good signal-to-noise ratios, but motions show a pattern of alternating upward and downward motions, indicated by the color scale, corresponding to the displacements seen in the enhanced electron density layers. The period of the oscillations is approximately 5 min in the early part of the night, decreasing to a few minutes later in the night.

[19] The image analysis can be applied to the CSR data to generate movie sequences that show the location and motion of the scatterers, as was done with the 14 June data. Three image frames are shown in Figures 11, 12, and 13. In the first image at 2329 UT, four lines of echoes can be seen over the western half of Puerto Rico. Although they are aligned approximately in the same direction as those observed on 14 June, i.e., west-northwest to east-southeast, the motion of the scatterers was toward north-northwest, in the direction opposite to that observed on 14 June. In the second figure at 2342 UT, two lines of echoes are still evident over the western part of Puerto Rico, but the echo structure west of the island has become more extended in the north-south direction. At this time, the two lines, which are the remnants of the structure in the first image frame,

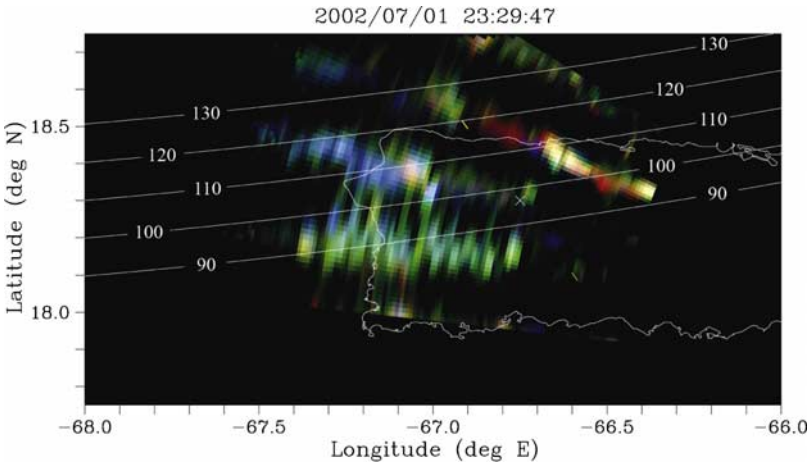

Figure 11. Map showing images obtained from the analysis of the coherent scatter measurements on 1 July 2002. The image in the figure corresponds to 2329 UT (AST + 4 hr).

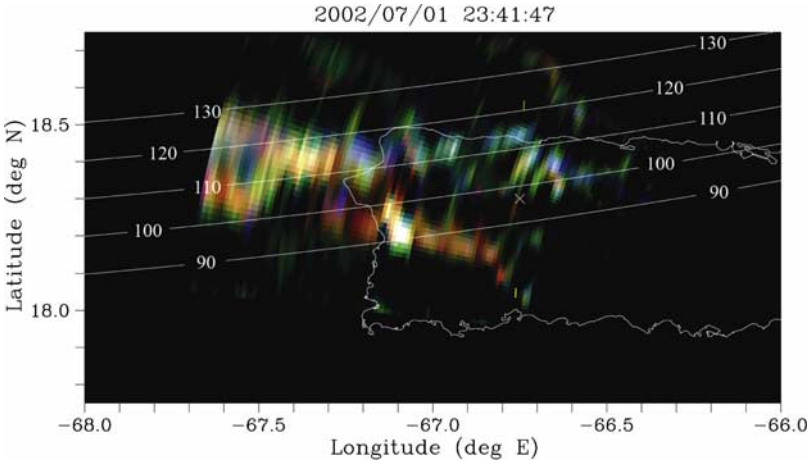

Figure 12. Map showing images obtained from the analysis of the coherent scatter measurements on 1 July 2002. The image in the figure corresponds to 2342 UT (AST + 4 hr).

were still moving in the north-northwest direction, but the structure further to the west was propagating eastward. In the third figure at 0232 UT, the echoes cover a smaller region and the separation between adjacent bands has decreased. The slopes in the CSR RTI are difficult to determine at this time and the sporadic *E* layer has become broader in altitude extent and weaker, as shown by the Arecibo ISR RTI.

2.3. 30 June 2002

[20] The CSR RTI for 30 June is shown in Figure 14. On this night, there were strong QP echoes prior to 0100 UT (2100 AST) but no discernible QP echoes later in the night. The slopes again show a mixture of toward and away directions throughout the period when the echoes were present, and there is a change in slopes from predominantly toward to predominantly away over a time of approximately 75 min. The ISR RTI, shown in Figure 15, shows only a weak sporadic *E* layer with relatively low densities in comparison with the layers on the two nights discussed above. The image frame obtained from the CSR data, in Figure 16, clearly shows that the echoes were located north and west of Arecibo, outside the area sampled by the ISR, which suggests that the layer may have been stronger and that the vertical layer displacements occurred in that region. This example shows that resolving and locating the echoes within the illuminated volume is important in the interpretation of the dynamics and electrodynamics associated with the sporadic layers and QP echoes. A simple RTI, such as that in Figure 14, would be difficult to interpret by itself when compared to the ISR measurements. The radar imaging results help to clarify the apparent discrepancy however.

3. Discussion and Conclusions

[21] In an earlier study, *Miller and Smith* [1978] also used the Arecibo 430-MHz ISR in an azimuth scanning mode to study the structure in sporadic *E* layers. Their scans were more restricted in azimuth, but the structure was similar to that seen in our observations. In particular, the horizontal scans in their study (see, e.g., their Figure 2) showed layering similar to that presented here and structures in the layers that were reminiscent of Kelvin-Helmholtz billow structure. *Miller and Smith* [1978] concluded that shear

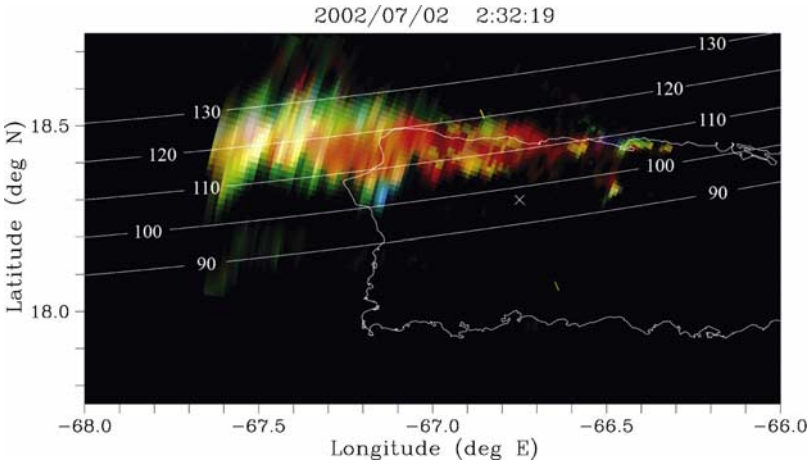

Figure 13. Map showing images obtained from the analysis of the coherent scatter measurements on 1 July 2002. The image in the figure corresponds to 0232 UT (AST + 4 hr).

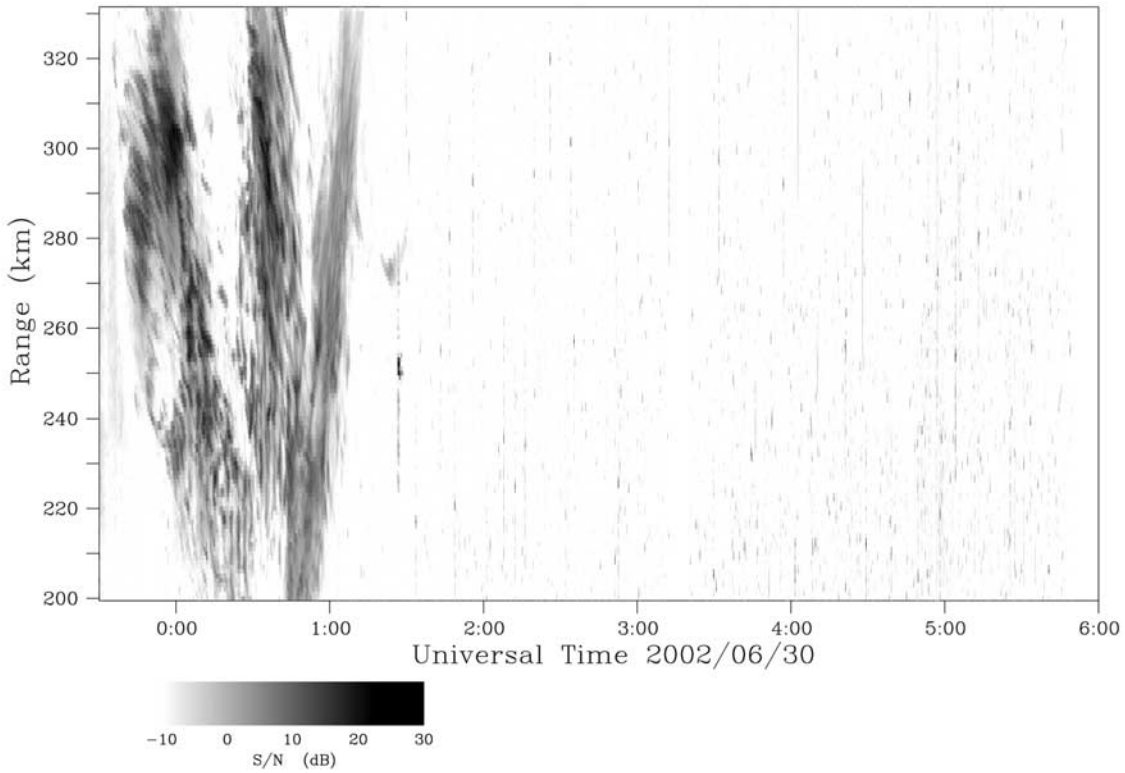

Figure 14. Coherent scatter radar RTI plot for the observations on the night of 30 June 30 to 1 July 2002.

instabilities in the neutral flow in the lower *E* region, and the associated billow structure were most likely responsible for the features that were observed.

[22] Another earlier study that is relevant here is the one by *Riggin et al.* [1986], which used azimuth scans obtained with the Arecibo ISR, as well as a coherent scatter very high frequency (VHF) radar located on St. Croix. The CSR was used for interferometry but did not have the receiving array required for the full imaging analysis that was applied in our study. The results showed electron density structures similar to those observed by *Miller and Smith* [1978] (see their Figure 4, for example) and by us. In addition, the scatterer centroid location obtained by interferometry from the St. Croix radar showed a pattern in which lines of echoes swept toward the radar and northward with increasing time in one case (see their Figure 6) and toward the radar and southward with increasing time in the other case (see their Figure 9). Their observations were therefore consistent with RTIs in which the echo line slopes were toward the radar in both cases, although the actual north/

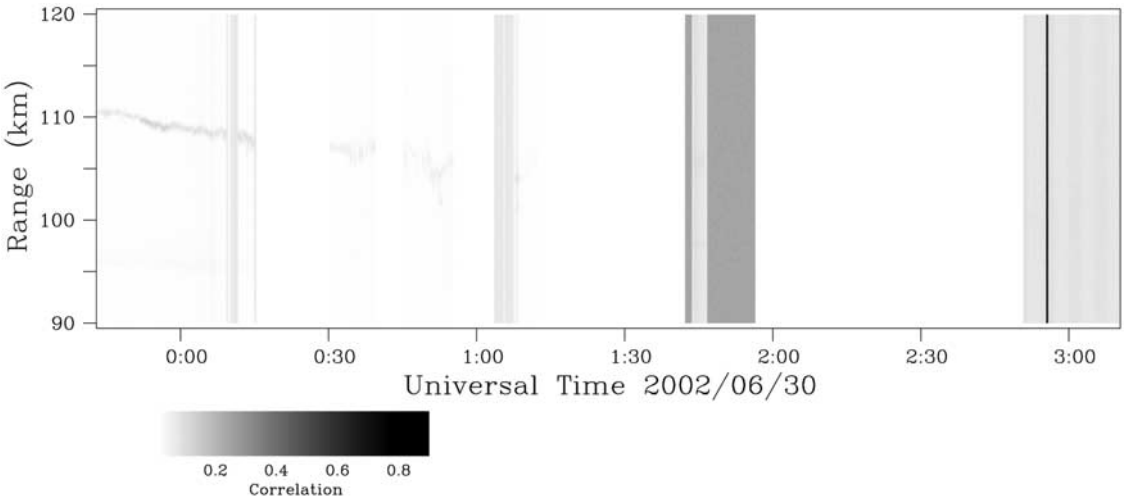

Figure 15. RTI measurements made with the incoherent scatter radar at Arecibo. The panel shows the pulse-to-pulse coherence.

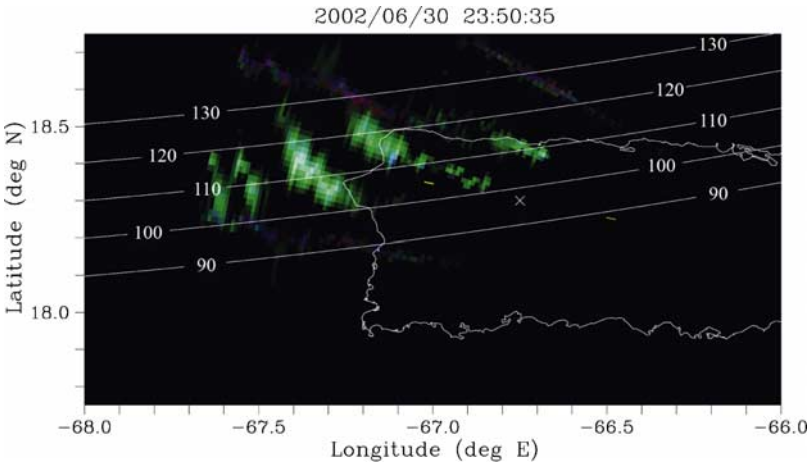

Figure 16. Map showing images obtained from the analysis of the coherent scatter measurements on 30 June 2002. The image in the figure corresponds to 2355 UT (AST + 4 hr).

south motion of the scatterers was reversed. As we have discussed in the previous sections, the imaging analysis that was applied to our data showed both types of cases, i.e., cases in which there was a southward propagation velocity component and cases in which there was a northward component. The horizontal scales and velocities observed by *Riggin et al.* [1986] were also consistent with the scales and velocities shown here.

[23] A more recent study by *Rosado-Roman et al.* [2004] used a similar setup again, with a VHF coherent scatter radar located on St. Croix to observe the *E* region volume above Arecibo. Their observations also showed structure that was consistent with that presented here.

[24] A number of studies of QP echoes have emphasized the dominant propagation direction toward the southwest or south-southwest. The study by *Saito et al.* [2005], for example, discusses that aspect of recent observations during the SEEK-2 campaign and also references many of the earlier papers that dealt with the propagation directions for the echo clusters. The preferred propagation direction has been used as evidence to support the theory developed by *Cosgrove and Tsunoda* [2004] that predicts a maximum growth rate for waves propagating in the southwest direction. Our data set is too small for meaningful statistics, but the imaging results show that, although the south-southwestward propagation direction is found frequently in the observations, other propagation directions are also common. As we have shown in the examples presented above, the direction in which the echo line structures move varies in the course of a given night and at times there are multiple structures moving in different directions at the same time within the region covered by the CSR.

[25] On the night of 14 June, we were able to obtain both the coherent and incoherent scatter radar data and imaging and lidar optical data during a strong QP event. The 557.7-nm all-sky images during the night showed structure in the airglow emissions with orientations, propagation directions, and propagation speeds that were consistent with those evident in the CSR imaging data. The green-line emission is a neutral emission generally centered near 95-km altitude, i.e., near the lower boundary of the sporadic *E* layer structures associated with the QP echoes. It is unlikely therefore that the optical images will consistently show the same structure as the radar, although there will be times when the plasma structures are low enough to overlap with the green-line emission layer. On 14 June that was the case, at least during part of the night, and there was a close correspondence between the neutral structures and the echo structures during those periods. Since the green-line emissions are associated with neutral processes, the close relationship between the two types of structures indicates that the plasma instabilities are ultimately driven by neutral dynamics.

[26] The potassium lidar data from the same night also suggests a neutral-driven process. The lidar measurements extend to higher altitudes and show vertical displacements that coincide with the vertical plasma displacements, but a vertical potassium layer displacement was also observed prior to the first ionization layer displacement. It therefore appears that neutral processes created a series of oscillations that were reflected in the vertical motion of the potassium and that the plasma responded after the neutrals were set in motion.

[27] As discussed by *Larsen* [2000], all of the sporadic *E* layer observations that have included neutral wind profile measurements have shown wind shears that were either unstable or very close to instability in the Kelvin-Helmholtz sense. The billow structure associated with the shear instability would have horizontal wavelengths and propagation velocities that are consistent with the range of periods and range rates that are typically found in coherent scatter RTIs. This suggests that the QP structures can be seeded by the neutral instabilities and that the source of energy for the plasma instabilities is the neutral processes. The theoretical results of *Rosado-Roman et al.* [2004] suggest that such a process can work, as do the simulations by *Bernhardt* [2002], which used a neutral Kelvin-Helmholtz instability as the driver for the *E* layer electrodynamics, to show that such a process could produce plasma structure consistent with the observations. The measurements made during the SEEK-2 experiment also support this point of view. Because of an unusual rocket trajectory, the chemical tracer

used to measure the winds was deployed along a more horizontal trajectory than is typically the case in the region where the sporadic *E* layer was located. The trail showed clear evidence of billow structure in the height range where large wind shears were measured [*Larsen et al.*, 2005]. Our observations do not exclude the possibility that the instability in the work of *Cosgrove and Tsunoda* [2004] plays a role in generating some of the echo structures that are observed; indeed, it may account for the slight bias in the observed propagation directions. The observations show, however, that other processes associated with the neutral dynamics are important and probably dominant in determining the orientation and propagation direction of the echo lines or patches.

[28] The QP echoes that we observed were localized, both horizontally and in the vertical. The echo structures often covered only a fraction of the volume illuminated by the CSR, so that the picture that emerges is one with larger patches with smaller-scale periodic echo structures embedded in those patches. As discussed in more detail by *Hysell et al.* [2004], use of the loci of perpendicularity is not sufficient to determine the altitude where the echoes originate. In that study, interferometry was used to show that the coherent echoes on 14 June were located in a relatively narrow range of altitudes that showed a general correspondence to but not an exact relation with the loci of perpendicularity (see their Figure 10 and 13). The observations from the additional nights presented here are consistent with those results in that the echoes appear to originate within the altitude range of enhanced electron densities associated with the sporadic *E* layer. In a recent study, *Saito et al.* [2006] detected echoes above 120-km altitude that occurred when QP structures were present, but the echoes were weak and the source of the echoes is not completely clear since they occur in an altitude range where the plasma densities are expected to be small.

[29] The observations presented here also show a close relationship between the uplift in the ionization layer measured with the ISR and the occurrence of coherent scatter echoes measured by the CSR.

[30] What is the source of the echoes then? In the early papers on the QP echo mechanism [e.g., *Woodman et al.*, 1991; *Tsunoda et al.*, 1994], the ordinary gradient drift instability was discounted as a likely explanation because the high conductivity parallel to the oblique magnetic field lines will strongly couple locally stable and unstable regions. The spatial resonance or special geometry requirements invoked in those early papers represented attempts to get around the coupling problem. More recent papers by *Hysell et al.* [2002a, 2002b], *Seyler et al.* [2004], and *Rosado-Roman et al.* [2004] have shown, however, that the simple picture is too limited and imposes unrealistic constraints. For the strong coupling model, the large conductivities parallel to the magnetic field **B** imply no variations along **B** and therefore wave numbers that are strictly perpendicular to the magnetic field. An unstable layer that is localized in height, however, requires that the wave number spectrum has a small but finite component parallel to the magnetic field lines. The studies cited above have shown that such solutions are not only possible but that the small parallel **k** component actually enhances the overall growth rate. The range of wavelengths where such solutions are possible is limited to a range with a large wavelength cut-off because of the more effective vertical electrical coupling at large spatial scales and a small wavelength cut-off due to viscous damping (see discussion in the work of *Rosado-Roman et al.* [2004], for example). This suggests therefore that the initiation of the instability is the vertical displacement generated by neutral atmosphere motions. The instabilities then occur where the ionosphere is locally unstable to gradient drift instability but with unstable modes that have a small but finite parallel wave number component. Since the components with a parallel wave number component have a higher growth rate, the instabilities that are localized in height are in fact also the instabilities that we should expect to observe.

[31] **Acknowledgments.** M. F. Larsen was partially supported by the National Science Foundation under grant ATM-0541593. D.L Hysell was partially supported by the National Science Foundation under grant ATM-0541526. The Arecibo Observatory is a major facility of the National Astronomy and Ionosphere Center, which is operated by Cornell University under a cooperative agreement with the National Science Foundation.

[32] Amitava Bhattacharjee thanks Peter Dyson and Susumu Saito for their assistance in evaluating this paper.

References

Bernhardt, P. A. (2002), The modulation of sporadic-E layers by Kelvin-Helmholtz billows in the neutral atmosphere, *J. Atmos. Sol.-Terr. Phys.*, *64*, 1487–1504.

Cosgrove, R. B., and R. T. Tsunoda (2004), Instability of the *E-F* coupled nighttime midlatitude ionosphere, *J. Geophys. Res.*, *109*, A04305, doi:10.1029/2003JA010243.

Hysell, D. L., and J. D. Burcham (1999), HF radar observations of quasi-periodic *E* layer echoes over North America, *J. Geophys. Res.*, *104*, 4361–4371.

Hysell, D. L., M. Yamamoto, and S. Fukao (2002a), Simulations of plasma clouds in the midlatitude *E* region ionosphere with implications for type I and type II quasiperiodic echoes, *J. Geophys. Res.*, *107*(A10), 1313, doi:10.1029/2002JA009291.

Hysell, D. L., M. Yamamoto, and S. Fukao (2002b), Imaging radar observations and theory of type I and type II quasi-periodic echoes, *J. Geophys. Res.*, *107*(A11), 1360, doi:10.1029/2002JA009292.

Hysell, D. L., M. F. Larsen, and Q. H. Zhou (2004), Common volume coherent and incoherent scatter radar observations of mid-latitude sporadic E-layers and QP echoes, *Ann. Geophys.*, *22*, 3277–3290, doi:1432-0576/ag/2004-22-3277.

Kane, T., B. Grime, S. Franke, E. Kudeki, J. Urbina, M. Kelley, and S. Collins (2001), Joint observations of sodium enhancements and field-aligned ionospheric irregularities, *Geophys. Res. Lett.*, *28*, 1375–1378.

Larsen, M. F. (2000), A shear instability seeding mechanism for quasiperiodic radar echoes, *J. Geophys. Res.*, *105*, 24,931–24,940.

Larsen, M. F., M. Yamamoto, S. Fukao, R. T. Tsunoda, and A. Saito (2005), Observations of neutral winds, wind shears, and wave structure during a sporadic- *E*/QP event, *Ann. Geophys.*, *23*, 2369–2375, doi:1432-0576/ag/2005-23-2369.

Miller, K. L., and L. G. Smith (1978), Incoherent scatter radar observations of irregular structure in mid-latitude sporadic *E* layers, *J. Geophys. Res.*, *83*, 3761–3775.

Pan, C. J., and M. F. Larsen (2000), Observations of QP radar echo structure consistent with neutral wind shear control of the initiation mechanism, *Geophys. Res. Lett.*, *27*, 867–870.

Riggin, D., W. E. Swartz, J. Providakes, and D. T. Farley (1986), Radar studies of long-wavelength waves associated with mid-latitude sporadic *E* layers, *J. Geophys. Res.*, *91*, 8011–8024.

Rosado-Roman, J. M., W. E. Swartz, and D. T. Farley (2004), Plasma instabilities observed in the E region over Arecibo and a proposed nonlocal theory, *J. Atmos. Sol.-Terr. Phys.*, *66*, 1593–1602, doi:10.1016/j.jastp.2004.07.005.

Saito, S., M. Yamamoto, S. Fukao, M. Marumoto, and R. T. Tsunoda (2005), Radar observations of field-aligned plasma irregularities in the SEEK-2 campaign, *Ann. Geophys.*, *23*, 2307–2318, doi:1432-0576/ag/2005-23-2307.

Saito, S., M. Yamamoto, H. Hashiguchi, and A. Maegawa (2006), Observation of three-dimensional structures of quasi-periodic echoes associated with mid-latitude sporadic-E layers by MU radar ultra-multi-channel system, *Geophys. Res. Lett.*, *33*, L14109, doi:10.1029/2005GL025526.

Seyler, C. E., J. M. Rosado-Roman, and D. T. Farley (2004), A nonlocal theory of the gradient-drift instability in the ionospheric E-region at mid-latitudes, *J. Atmos. Sol.-Terr. Phys.*, *66*, 1627–1637.

Taylor, M. J., S. H. Seo, T. Nakamura, T. Tsuda, H. Fukunishi, and Y. Takahashi (1998), Long base-line measurements of short-period mesospheric gravity waves during the SEEK campaign, *Geophys. Res. Lett.*, *25*, 1797–1800.

Tsunoda, R. T., S. Fukao, and M. Yamamoto (1994), On the origin of quasi-periodic radar backscatter from mid-latitude sporadic E, *Radio Sci.*, *29*, 349.

Woodman, R. F., M. Yamamoto, and S. Fukao (1991), Gravity wave modulation of gradient drift instabilities in mid-latitude sporadic E irregularities, *Geophys. Res. Lett.*, *18*, 1197.

Yamamoto, M., S. Fukao, R. F. Woodman, T. Ogawa, T. Tsuda, and S. Kato (1991), Midlatitude *E* region field-aligned irregularities observed with the MU radar, *J. Geophys. Res.*, *96*, 15943–15949.

Yamamoto, M., S. Fukao, T. Ogawa, T. Tsuda, and S. Kato (1992), A morphological study on mid-latitude E-region field-aligned irregularities observed with the MU radar, *J. Atmos. Terr. Phys.*, *54*, 769.

R. L. Bishop, The Aerospace Corporation, Los Angeles, CA, USA.

J. Friedman, The Arecibo Observatory, Arecibo, Puerto Rico.

D. L. Hysell, Earth and Atmospheric Sciences, Cornell University, Ithaca, NY, USA.

M. F. Larsen, Department of Physics and Astronomy, Clemson University, Clemson, SC 29634, USA. (mlarsen@clemson.edu)

S. M. Smith, Center for Space Physics, Boston University, Boston, MA, USA.

Q. H. Zhou, Electrical and Computer Engineering Department, Miami University, Oxford, OH, USA.